

1 **Incorporating genome-based phylogeny and trait similarity into diversity assessments**
2 **helps to resolve a global collection of human gut metagenomes**

3 Nicholas D. Youngblut^{*,1}, Jacobo de la Cuesta-Zuluaga¹, Ruth E. Ley¹
4 ¹Department of Microbiome Science, Max Planck Institute for Developmental Biology, Max
5 Planck Ring 5, 72076 Tübingen, Germany

6 * Corresponding author: Nicholas Youngblut

7 **Running title:** Phylogeny and traits explain metagenome diversity

8 **Key words:** human gut, metagenome, phylogeny, traits, diversity

9 Abstract

10 Tree-based diversity measures incorporate phylogenetic or phenotypic relatedness into
 11 comparisons of microbial communities. This improves the identification of explanatory factors
 12 compared to tree-agnostic diversity measures. However, applying tree-based diversity
 13 measures to metagenome data is more challenging than for single-locus sequencing (e.g., 16S
 14 rRNA gene). The Genome Taxonomy Database (GTDB) provides a genome-based reference
 15 database that can be used for species-level metagenome profiling, and a multi-locus phylogeny
 16 of all genomes that can be employed for diversity calculations. Moreover, traits can be inferred
 17 from the genomic content of each representative, allowing for trait-based diversity measures.
 18 Still, it is unclear how metagenome-based assessments of microbiome diversity benefit from
 19 incorporating phylogeny or phenotype into measures of diversity. We assessed this by
 20 measuring phylogeny-based, trait-based, and tree-agnostic diversity measures from a large,
 21 global collection of human gut metagenomes composed of 33 studies and 3348 samples. We
 22 found phylogeny- and trait-based alpha diversity to better differentiate samples by
 23 westernization, age, and gender. PCoA ordinations of phylogeny- or trait-based weighted
 24 UniFrac explained more variance than tree-agnostic measures, which was largely a result of
 25 these measures emphasizing inter-phylum differences between *Bacteroidaceae* (*Bacteroidota*)
 26 and *Enterobacteriaceae* (*Proteobacteria*) versus just differences within *Bacteroidaceae*
 27 (*Bacteroidota*). The disease state of samples was better explained by tree-based weighted
 28 UniFrac, especially the presence of Shiga toxin-producing *E. coli* (STEC) and hypertension. Our
 29 findings show that metagenome diversity estimation benefits from incorporating a
 30 genome-derived phylogeny or traits.

31 Importance

32 Estimations of microbiome diversity are fundamental to understanding spatiotemporal
 33 changes of microbial communities and identifying which factors mediate such changes.
 34 Tree-based measures of diversity are widespread for amplicon-based microbiome studies due
 35 to their utility relative to tree-agnostic measures; however, tree-based measures are seldomly
 36 applied to shotgun metagenomics data. We evaluated the utility of phylogeny-, trait-, and
 37 tree-agnostic diversity measures on a large scale human gut metagenome dataset to help guide
 38 researchers with the complex task of evaluating microbiome diversity via metagenomics.

39 Introduction

40 Sequencing-based assessments of microbiome diversity are fundamental to the field of
 41 microbiome science. For instance, 16S rRNA gene and metagenomic sequence-based
 42 estimations of human gut microbiome diversity have shown substantial differences among
 43 individuals due to disease state, diet, exercise, hygiene, and antibiotic usage (Sommer and
 44 Bäckhed, 2013). The choice of diversity measure can be critical, as exemplified in many studies
 45 where only diversity assessments that incorporated microbial phylogenetic relatedness were

discriminatory, while tree-agnostic diversity measurements could not distinguish between groupings (Bassett *et al.*, 2015; Obregon-Tito *et al.*, 2015; Vogt *et al.*, 2017; Torres *et al.*, 2018). Without incorporating a phylogeny, all microbes in a community are treated as equally related (*i.e.*, a star phylogeny), so within-genus differences in species composition are weighted the same as compositional differences spanning multiple phyla or domains (Matsen, 2015). Closely related species are often phenotypically similar and occupy comparable niches; therefore, a measure of diversity that incorporates phylogenetic information can indirectly assess functional overlap among microbial communities (Lozupone and Knight, 2008). Such an approach is quite powerful, considering that the majority of microbes remain uncultured, and that the common approach of 16S rRNA gene sequencing can only provide coarse inferences of phenotype due to the lack of taxonomic resolution (Hugerth and Andersson, 2017; Louca, Doebeli and Parfrey, 2018). Still, trait-based assessments of microbiome diversity that focused on a few key phenotypes have been employed with great effect in some circumstances (Ortiz-Álvarez *et al.*, 2018; Guittar, Shade and Litchman, 2019). More generally, phylogeny-based measures of within-sample and between-sample diversity (alpha and beta diversity, respectively) have become commonplace for microbiome studies relying on 16S rRNA sequencing (Lozupone and Knight, 2008; Hamady, Lozupone and Knight, 2010).

As the cost of sequencing has declined, shotgun metagenomics has risen in popularity relative to single-locus sequencing, as metagenomics provides a great wealth of information, including i) accurate species-level taxonomic classification and abundance estimation, ii) information on gene and metabolic pathway content, and iii) the ability to assemble genes and metagenome-assembled genomes (MAGs) (Lu *et al.*, 2017; Parks *et al.*, 2017; Franzosa *et al.*, 2018). Recent work has shown that shallow sequencing depths can provide similar or greater coverage of microbial diversity compared to 16S rRNA sequencing (Hillmann *et al.*, 2018). However, generating a phylogeny from shotgun metagenome data is inherently challenging, since read sequences originate from all genomic locations instead of a single locus (Kembel *et al.*, 2011). Various methods exist for extracting 16S rRNA gene sequences, other single loci, or multi-locus data from metagenome reads (*e.g.*, EMIRGE, MATAM, AMPHORA2, PhyloSIFT, and MetaPhlAn2), but this excludes much of the data, limiting the detection sensitivity for less common taxa (Miller *et al.*, 2011; Segata *et al.*, 2012; Wu and Scott, 2012; Darling *et al.*, 2014; Pericard *et al.*, 2018). Alternatively, assembling MAGs enables the construction of multi-locus phylogenies from all assembled genomes, but a very high sequencing depth is required to assemble even the majority of taxa in a diverse microbial community like in soil or the human gut. Another approach is to map all reads to a database of entire genomes (*e.g.*, GenBank or RefSeq), which increases the amount of reads classified relative to single- or multi-locus approaches, but such databases generally lack careful curation of genome assembly quality, a standardized taxonomy, and multi-locus phylogenies for all reference genomes (Parks *et al.*, 2018).

We recently created a pipeline for generating custom metagenome profiling databases from the Genome Taxonomy Database (GTDB) (Parks *et al.*, 2018; de la Cuesta-Zuluaga, Ley and Youngblut, 2019), which is a comprehensive database of *Bacteria* and *Archaea* genomes, that not only provides a coherent microbial taxonomy based on genome relatedness, but it also includes multi-locus genome phylogenies for the reference species. Therefore, one can map all

reads to the GTDB reference genomes in order to infer species-level abundances (e.g., with Kraken2) and then utilize a genome phylogeny of reference species for calculating alpha and beta diversity (Wood, Lu and Langmead, 2019). Importantly, the multi-locus genome phylogeny will almost definitely be more robust and better-resolved than a phylogeny inferred from small, hypervariable regions of the 16S rRNA gene, or even the full-length gene sequence (Maiden *et al.*, 1998). Using species-level reference genomes also enables trait inference directly from the loci present in each genome, which is a task that state-of-the-art classifiers can perform accurately, at least for certain common phenotypes such as cell morphology, anaerobiosis, spore formation, and utilization of certain carbohydrates (Weimann *et al.*, 2016). Trait relatedness can then be represented in a tree format by hierarchical clustering of genomes based on trait presence/absence to produce a dendrogram.

While promising, this approach of species-level metagenome profiling, followed by phylogeny- or trait-based diversity calculation has not been robustly assessed and compared to tree-agnostic approaches that are often used for shotgun metagenome studies. We therefore applied this methodology to a large, global human gut metagenome collection, comprising 33 datasets and 3348 samples. We found that, in comparison to tree-agnostic measures, both phylogeny- and trait-based measures of alpha and beta diversity improved our ability to discriminate metagenome samples based on westernization, disease status, age, and gender.

Methods

Data Retrieval

We retrieved publicly available human gut metagenomes from the Sequence Read Archive (SRA) between December 2019 and February 2020 (Table S1). Sample metadata was obtained from the curatedMetagenomicData v.1.17.0 Bioconductor package (Pasolli *et al.*, 2017) and included according to the following criteria: i) shotgun metagenomes sequenced using the Illumina HiSeq platform with a median read length >95 bp; ii) with available SRA accession; iii) labeled as adults or seniors, or with a reported age ≥18 years; iv) without report of antibiotic consumption (*i.e.*, no or NA); v) without report of pregnancy (*i.e.*, no or NA); vi) non-lactating women (*i.e.*, no or NA); vii) without report of gangrene, pneumonia, cellulitis, adenoma, colorectal cancer, arthritis, Behcet's disease, cirrhosis or inflammatory bowel disease. Only forward reads were downloaded and further processed. The final dataset was composed of 3348 samples from 33 studies.

Sequence processing and taxonomic profiling

We used the bbtools “bbduk” command and Skewer v0.2.2 (Jiang *et al.*, 2014) to trim adapters and quality-filter raw sequences. The “bbmap” command from bbtools was used to remove human reads mapping to the human genome hg19 assembly. We created quality reports for each step using fastqc v0.11.7 (<https://github.com/s-andrews/FastQC>) and multiQC v.1.5a (Ewels *et al.*, 2016). Filtered reads were subsampled to 1 million reads per sample and used to obtain taxonomic profiles using Kraken2 (Wood, Lu and Langmead, 2019) and Bracken v2.2 (Lu *et al.*, 2017). Custom databases of Bacteria and Archaea were created using Struo

v0.1.6 (de la Cuesta-Zuluaga, Ley and Youngblut, 2019) and based on the Genome Taxonomy Database (GTDB), Release 89.0 (“GTDB-r89”; available at <http://ftp.tue.mpg.de/ebio/projects/struo/>) (Parks *et al.*, 2018).

Genome phylogeny

The GTDB-r89 “Arc122” and “Bac120” multi-locus phylogenies were obtained from the GTDB ftp server (<https://data.ace.uq.edu.au/public/gtdb/data/releases/release89/>). The ape R package was used to merge the trees and prune them to the 23,360 species in the Struo-generated GTDB-r89 metagenome profiling database.

Trait inference

We generated a Python v3 implementation of traitar (Weimann *et al.*, 2016) and used it to predict traits for all genomes (<https://github.com/nick-youngblut/traitar3>), with majority-rules (phypat+PGL model) used for classifying trait presence/absence. We used the vegan R package (Oksanen *et al.*, 2012) to apply the Jaccard dissimilarity metric to the binary traits-per-genome matrix in order to create a distance matrix of trait relatedness among genomes. This distance matrix was clustered via the UPGMA algorithm to create a dendrogram, which was used for tree-based alpha and beta diversity metrics.

Congruence of the genome phylogeny and trait similarity

Global congruence of the genome phylogeny and trait similarity dendrogram was assessed via phytools::cospeciation with 100 permutations for the null model. Local congruence (*i.e.*, per-clade) was assessed via Procrustes superimposition (vegan::procrustes) comparing the genome phylogeny patristic distance matrix versus the Jaccard distance matrix used to generate the trait similarity dendrogram. Due to memory limitation issues with the standard approach for converting a phylogeny to a patristic distance matrix in R (*i.e.*, the “cophenetic” function in the ape R package can only process trees with fewer than ~13,000 tips), we instead ran the procrustes analysis on 1000 randomly pruned subtrees of 1000 tips each and used the mean residuals across all permutations for each taxon.

Alpha diversity

We calculated tree-agnostic (species richness and Shannon index) and tree-based (Faith’s Phylogenetic Diversity: Faith’s PD) alpha diversity measures. Species richness and Shannon index. All tree-agnostic measures were calculated with the vegan R package (vegan::diversity), and Faith’s PD was calculated with PhyloMeasures::pd.query. The lme4 and lmerTest R packages were used to fit linear mixed effects models with dataset as random effect and other variables as fixed effects; *F*-tests and *P*-values were determined via the Satterthwaite’s method (ANOVA Type II sum of squares). We adjusted *P*-values for multiple comparisons using the Benjamini-Hochberg method.

163 *Beta diversity analyses*

164 Tree-agnostic weighted and unweighted intersample distances (Bray-Curtis dissimilarity
165 and Jaccard index) were calculated using the vegan R package (vegan::vegdist), while
166 tree-based metrics (weighted and unweighted UniFrac) were calculated with rbiom::unifrac.
167 Principal coordinates analysis (PCoA) was applied to each distance matrix via stats::cmdscale.
168 We used the vegan::envfit function to assess correlations of species abundances to each PCoA.
169 PERMANOVA was performed with vegan::adonis2 (999 permutations; marginal effects of terms
170 assessed). We assessed PCoA ordination similarity via Procrustes superimposition (999
171 permutations).

172 *General data analysis*

173 General data processing was performed with the tidyverse package in R. The ggplot2
174 package was used for generating all plots. All code used for this work is available on GitHub at
175 https://github.com/leylabmpi/global_metagenome_diversity.

176 *Data availability*

177 The genome phylogeny, trait tables for each species-genome representative, and trait
178 dendrograms are available at http://ftp.tue.mpg.de/ebio/projects/struo/GTDB_release89/.

179 *Results*

180 *Dataset summary*

181 Our combined human gut metagenome dataset consisted of 33 studies and a total of
182 3348 samples from 3011 individuals after filtering by required metadata fields and an adequate
183 number of reads following quality control (101 ± 163 s.d. samples per study; Figure S1A). The
184 percent of metagenome reads classified to our custom GTDB-r89 Kraken2 database was high
185 (mean of 80%), and generally lowest for non-westernized populations (Figure S1B).

186 *Broad-scale incongruences between trait and phylogenetic similarity*

187 To assess alpha and beta diversity based on phenotypic similarity, we inferred the
188 presence/absence of 67 traits for each reference genome in our Kraken2 database (Figure 1A).
189 We quantified the degree of congruence between phylogeny- and trait-based relatedness of all
190 species (taxonomy defined by the GTDB), in order to assess whether each would reveal
191 different patterns of alpha and beta diversity. Congruence was measured via Procrustes
192 superimposition, in which larger incongruences between phylogenetic and trait similarity among
193 taxa will produce larger Procrustes residuals. We found that the congruence between trait and
194 phylogenetic similarity differed greatly across phyla (Figure 1B). The bacterial phyla
195 *Dependentiae*, *Fusobacteriota*, and *Verrucomicrobiota_A* were the most congruent between trait
196 and phylogenetic similarity, while most of the archaeal phyla, including the *Crenarcheota*,

197 *Thermoplasmatota*, and *Nanoarchaeota* were the most incongruent. Notably, *Crenarcheota*
198 were also found in a recent study to be especially variable in phenotypes, as defined by overlap
199 in clusters of orthologous groups (COG) functional categories (Royalty and Steen, 2019).
200 *Firmicutes* and *Proteobacteria* showed the greatest variance in congruence, with many highly
201 incongruent outlier species in both phyla. An inspection at the family level revealed that the
202 *Firmicutes* outliers belonged to *Enterobacteriaceae*, while the *Mycoplasmoidaceae* and
203 *Metamycoplasmataceae* families were the largest outliers in *Proteobacteria* (Figure S2).
204 *Euryarchaeota* trait-phylogeny congruence was relatively high for an archaeal phylum; however,
205 the *Methanosphaera* genus comprised many highly incongruent outliers. Large differences
206 between phylogeny and phenotype in these families may be due to high phenotypic plasticity
207 relative to core genome evolutionary rates. Overall, our findings show that trait and phylogenetic
208 similarities are only partially congruent and would thus likely describe different aspects of
209 microbiome diversity when applied to tree-based diversity measures.

210 *More variance is explained by alpha diversity measures incorporating phylogenetic or trait* 211 *relatedness*

212 We calculated alpha diversity for all 3348 metagenome samples with four measures: the
213 number of observed taxa, the Shannon Index, and Faith's Phylogenetic Diversity (Faith's PD)
214 with either the genome phylogeny ("PD_phy") or a dendrogram depicting trait relatedness
215 ("PD_trt"). We note that all metagenomes were subsampled to 1 million reads prior to
216 metagenome profiling and thus alpha diversity estimates should not be biased by sampling
217 depth. Both PD_phy and PD_trt clearly separated metagenome samples based on
218 westernization status, while such a separation was less discernible when using the Shannon
219 Index or number of observed species (Figure 2A). When assessing samples with westernization
220 status, age, and gender metadata ($n = 1843$), we also found that PD_phy and PD_trt more
221 clearly differentiate groups along each variable (Figure 2B). Indeed, linear mixed effects models
222 produced substantially higher and lower F -values and P -values, respectively, for PD_phy and
223 PD_trt in regards to westernization status, age, and gender (Figure 2C). F -values were also
224 slightly higher for BMI when filtering the dataset to just samples with all required metadata ($n =$
225 918; Figure 2C). PD_phy F -values were consistently higher for age and especially for
226 westernization compared to PD_trt. Indeed, the number of phyla per sample was substantially
227 higher for non-westernized individuals versus westernized (Figure S3A), while no substantial
228 difference was seen for the number of genera (Figure S3B). This finding indicates that coarse
229 taxonomic groups differ substantially by westernization status, which would be emphasized via
230 a phylogenetic measure of diversity. While the boxplots hinted at a substantially greater
231 differentiation between westernized and non-westernized males versus when comparing
232 females (Figure S3B), we did not find a significant interaction between gender and
233 westernization for any diversity measure ($P > 0.1$).

234 To resolve how the choice of diversity measure influenced per-clade estimations of
235 diversity, we applied our mixed effects model analysis on alpha diversity calculated for each
236 individual family (Figure S4). For all diversity measures, the *Bacteroidales* family F082 was most
237 strongly associated with westernization status, and the strength of association was very

consistent among measures. In contrast, most of the other families associated with westernization differed in their strength among the diversity measures (Figure S4A). For instance, the association of *Treponemataceae* was substantially weaker for the Shannon Index versus either tree-based measure. This inconsistency among diversity measures was also observed for associations between family-level diversity and gender or age. *Akkermansiaceae* had the strongest association with gender, but only for Faith's PD based on trait similarity (Figure S4B), suggesting functional differentiation at fine taxonomic levels. Notably, *Methanobacteriaceae* alpha diversity was most strongly associated with age, along with *Butyricicoccaceae*, but the association strength was much lower when measuring diversity via PD_phy versus PD_trt or the Shannon index (Figure S4C). These examples show that fine taxonomic level diversity estimations can differ substantially depending on which aspects of diversity are emphasized: phylogenetic relatedness, trait relatedness, or neither.

More variance is explained by beta diversity measures incorporating phylogenetic or trait relatedness

We calculated beta diversity on all metagenome samples with 6 metrics: Bray Curtis, Jaccard, and UniFrac in all four combinations of unweighted and weighted with either a genome phylogeny or trait-similarity dendrogram. Principal coordinate analysis (PCoA) revealed that substantially more variance was explained by the top principle coordinates (PCs) for both phylogeny-based weighted UniFrac ("w-unifrac_phy") and trait-based weighted UniFrac ("w-unifrac_trt") (Figure 3). This was especially apparent for w-unifrac_phy, with 50% variance explained by PC1 alone, while only 15.4 and 9.3% variance was explained by PC1 for Bray-Curtis and Jaccard, respectively (Figure 3B). In contrast to weighted UniFrac, both unweighted UniFrac measures showed similar amounts of variance explained relative to Bray-Curtis and Jaccard. When summing across the top 5 PCs (Figure 3C), w-unifrac_phy explained 79.1% of the variance, which is more than twice that of Bray-Curtis (38.2%) and more than three times as much as Jaccard (23.8%). The summed percent variance explained by w-unifrac_trt was also substantially higher (53.3%) than Bray-Curtis and Jaccard.

We investigated why w-unifrac_phy and w-unifrac_trt explained so much more variance by correlating species abundances with each of the top three PCs (Figure 4A). The analysis revealed that the top w-unifrac_phy and w-unifrac_trt PCs most strongly differentiates samples based on the abundances of species belonging to *Lachnospiraceae* (*Firmicutes_A*), *Bacteroidaceae* (*Bacteroidota*), and *Enterobacteriaceae* (*Proteobacteria*). In contrast, Bray-Curtis and Jaccard most strongly discern samples differing in species just within *Bacteroidaceae* (*Bacteroidota*). Specifically, the top PCs for Bray-Curtis and Jaccard correlate strongly with the *Bacteroidaceae* genera: *Bacteroidetes*, *Bacteroidetes_B*, and *Prevotella* (Figure S5). Unlike the weighted UniFrac measures, both unweighted UniFrac measures lacked a strong correlation with *Enterobacteriaceae*, but they did uniquely discern *Oscillospiraceae* (*Firmicutes_A*) and *Ruminococcaceae* (*Firmicutes_A*).

To help illustrate these clade-level differences among the beta diversity measures, we mapped the abundances of these focal clades onto each PCoA ordination. As denoted by our

correlation analysis, *Bacteroidaceae* was highly abundant at both ends of PC1 for Bray-Curtis and Jaccard, while its abundance was lowest at the center of the PC (Figure 4B). Conversely, *Bacteroidaceae* was only highly abundant on one side of PC1 for both w-unifrac_phy and w-unifrac_trt. In contrast to *Bacteroidaceae*, *Enterobacteriaceae* was only detectable in 350 samples, with only 28 samples having >1% abundance (Figure 4C). w-unifrac_trt best partitioned the samples with high versus low levels of *Enterobacteriaceae* (Figure 4A & 4C), while w-unifrac_phy also partitioned these samples well, especially along PC2. Plotting *Lachnospiraceae*, *Oscillospiraceae*, and *Ruminococcaceae* abundances on the PCoA ordinations did confirm the correlation analysis, in which *Lachnospiraceae* abundance correlates rather well with PC1 and PC2 of all ordinations, while the *Oscillospiraceae* and *Ruminococcaceae* abundances best correlate the the top PCs for both unweighted UniFrac measures (Figure S6).

We also correlated alpha diversity with the PCoA PCs but found substantially weaker associations ($R^2 < 0.21$ for all measures). Still, gradients of diversity are somewhat apparent across the ordinations, regardless of the diversity measure (Figure S7).

To determine how well each beta diversity measure partitions individuals by age, gender, BMI, westernization, and disease states, we performed PERMANOVA with each measure on all samples with the requisite metadata ($n = 1413$). Although all model variables were significant due to the large sample size ($P < 0.001$), the effect sizes varied considerably for disease state and westernization (Figure 5). Most notably, w-unifrac_phy had an R^2 for disease state that was about twice that of Bray-Curtis or Jaccard (0.082 versus 0.041 and 0.025, respectively). Plotting the location of each metagenome sample from each disease category on PC1 illustrated how Bray-Curtis and Jaccard largely relegate most samples with each disease state to the same half of PC1, while “healthy” samples span the entire PC (Figure 5B). In contrast, the UniFrac measures, especially the weighted versions, partition the various disease states into different regions along the entire length of the PC.

To directly quantify the differences in how each beta diversity measure partitioned samples in each disease category, we performed pairwise Procrustean superposition analyses between each beta diversity measure. Large Procrustes residuals for a disease state indicate that the relative positions of samples in that grouping differ greatly between the two PCoA ordinations. Procrustes residuals were highest for Shiga toxin-producing *E. coli* (STEC) and hypertension disease states when comparing the UniFrac measures to Bray-Curtis or Jaccard (Figure S8). STEC was also moderately divergent between the trait-based and phylogeny-based UniFrac measures (both weighted and unweighted). This discrepancy between diversity measures reflects the incongruence between phylogeny- and trait-based relatedness among *Enterobacteriaceae* species (Figure S2).

Discussion

Shotgun metagenomics will continue to increase in popularity as the cost of sequencing declines and methods for processing and interpreting metagenomic data continue to develop. A major challenge is to fully harness the heterogeneous sequence data generated by metagenomics, which is vastly more complex than 16S rRNA gene sequences or other

single-locus datasets. Measuring community diversity from such heterogeneous data is not straight-forward, and it is often unclear what measures of diversity are most appropriate for metagenome data. Here, we have assessed a method of microbiome diversity measurement by using metrics that incorporate a multi-locus phylogeny or a large set of traits inferred from reference genomes to species-level abundance profiles mapped against species-level genome representatives from the GTDB. Our method is not computationally demanding, generalizable to a wide range of microbiome studies, and flexible in regards to which tree-based measures and which traits are used.

We have shown that our tree-based diversity measures explained more variance, both in regards to overall inter-sample diversity and diversity among individuals differing in westernization, age, gender, and disease status (Figures 2 & 3). While BMI seemed to be slightly better explained by phylogeny- and trait-based measures, the difference was too small to be conclusive. Interestingly, westernization was substantially better explained by the phylogeny-based alpha diversity measure relative to all other measures, while this pattern was not observed for beta diversity. These results suggest that while overall phylogenetic diversity is greater for non-westernized individuals, there is enough broad-scale phylogenetic overlap between individuals to appear highly similar in a direct comparison.

We additionally showed that phylogeny and trait-based diversity measures were more explanatory than tree-agnostic measures due to how each underscored different aspects of community diversity (Figure 4). Bray-Curtis and Jaccard emphasized compositional differences within the *Bacteroidaceae*, which is a prevalent and relatively abundant clade in the human gut. Instead, both the phylogeny and trait-based measures accentuated differences between *Enterobacteriaceae* and *Bacteroidaceae*, which not only belong to different phyla, but also the former is much less prevalent than the latter. This emphasis on *Enterobacteriaceae* by the tree-based diversity measures likely explains why the disease state that differed most between PCoA ordinations was Shiga toxin-producing *E. coli* (Figure S8). The same may be true for the presence of hypertension, which was the second-most different between PCoA ordinations, as the *Enterobacteriaceae* genus *Klebsiella* has been found to overgrow in hypertensive individuals (Li *et al.*, 2017). Of course, this increased emphasis on *Enterobacteriaceae* by the tree-based measures is just the most prominent, and as we observed for our family-level assessment of alpha diversity, many clades can differ in their apparent diversities depending on the measure used.

In almost all circumstances, phylogeny-based diversity was more explanatory than when incorporating trait relatedness. Our assessment of congruence between phylogenetic and trait-based similarity showed why these diversity measures would differ. For instance, the lower explanatory power of trait-based diversity in regards to disease state can be attributed to the incongruence between trait and phylogeny for many species in the *Enterobacteriaceae* family (Figures 5 & S2) or possibly to the choice of traits included (Figure 1). While we did use a large number of traits relative to other recent trait-based studies of microbial community spatiotemporal diversity (Ortiz-Álvarez *et al.*, 2018; Guittar, Shade and Litchman, 2019), they are likely just a minor subset of all relevant phenotypes. Traits could be defined more abstractly as COG functional categories, KEGG pathways, or other broad classifications of gene function, which may generalize better to novel microbial genetic diversity compared to using a trait

classifier trained on a subset of all known microbial species (Royalty and Steen, 2019). However, broad and generalized demarcations of function may obscure particular traits that are most strongly varying across the spatiotemporal gradient of interest. One could choose particular functional categories, like the gut-brain modules defined in a recent study for understanding microbial functional interaction with mental health (Valles-Colomer *et al.*, 2019), although the expert knowledge required to make such targeted selections is often lacking for many systems.

We must note that our method of predicting traits based on the presence of loci presumably produced false negatives for poorly studied clades in which novel genetic mechanisms generate the same phenotypes. Given that the gut microbiome is dominated by a few relatively well-studied clades (Lloyd-Price *et al.*, 2017), the impact of false negatives was likely small for our trait-based weighted UniFrac measure but may have been higher for unweighted UniFrac. Still, both phylogeny- and trait-based unweighted UniFrac were less explanatory than their weighted counterparts, suggesting that inaccuracies in our trait classification approach were negligible. Advances in machine learning models for predicting gene annotations, protein structure and interactions, and metabolic pathways will improve classification of specific microbial phenotypes, especially when generalizing to novel genetic diversity (Celesti *et al.*, 2018; Bileschi *et al.*, 2019).

While our findings demonstrate the potential benefit of incorporating phylogeny or function based on genome representatives of each reference species, much is still unknown about how best to implement these approaches across highly varied microbiome studies. Function-based diversity measures may prove to be highly advantageous for studies of microbial community succession, as some studies have demonstrated (Ortiz-Álvarez *et al.*, 2018; Guittar, Shade and Litchman, 2019). Microbiomes with high numbers of uncultured species such as seafloor sediments may benefit from using a more generalized measure of traits like COG functional categories (Orsi, 2018). We recommend a focus on phylogeny-based diversity measures for shotgun metagenomics data in cases where the most informative traits are unknown, since phylogenetic information will be relevant for most if not all systems, and it will allow for direct cross-study comparisons of microbial diversity.

Author contributions

Author contributions: N.D.Y. and J.dlC. designed the research; N.D.Y. and J.dlC. performed research; N.D.Y. analyzed data; and N.D.Y., J.dlC., and R.E.L. wrote the paper.

Acknowledgements

We thank Albane Ruaud and Taichi Suzuki for providing important feedback on this work.

Funding

This work was supported by the Max Planck Society.
Conflict of Interest: none declared.

399 References

- 400 Bassett, S. A. *et al.* (2015) 'Changes in composition of caecal microbiota associated with
401 increased colon inflammation in interleukin-10 gene-deficient mice inoculated with *Enterococcus*
402 species', *Nutrients*, 7(3), pp. 1798–1816. doi: 10.3390/nu7031798.
- 403 Bileschi, M. L. *et al.* (2019) 'Using Deep Learning to Annotate the Protein Universe', *bioRxiv*.
404 doi: 10.1101/626507.
- 405 Celesti, F. *et al.* (2018) 'Why Deep Learning Is Changing the Way to Approach NGS Data
406 Processing: A Review', *IEEE reviews in biomedical engineering*, 11, pp. 68–76. doi:
407 10.1109/RBME.2018.2825987.
- 408 de la Cuesta-Zuluaga, J., Ley, R. E. and Youngblut, N. D. (2019) 'Struo: a pipeline for building
409 custom databases for common metagenome profilers', *Bioinformatics* . doi:
410 10.1093/bioinformatics/btz899.
- 411 Darling, A. E. *et al.* (2014) 'PhyloSift: phylogenetic analysis of genomes and metagenomes',
412 *PeerJ*, 2, p. e243. doi: 10.7717/peerj.243.
- 413 Ewels, P. *et al.* (2016) 'MultiQC: summarize analysis results for multiple tools and samples in a
414 single report', *Bioinformatics* , 32(19), pp. 3047–3048. doi: 10.1093/bioinformatics/btw354.
- 415 Franzosa, E. A. *et al.* (2018) 'Species-level functional profiling of metagenomes and
416 metatranscriptomes', *Nature methods*, 15(11), pp. 962–968. doi: 10.1038/s41592-018-0176-y.
- 417 Guittar, J., Shade, A. and Litchman, E. (2019) 'Trait-based community assembly and succession
418 of the infant gut microbiome', *Nature communications*, 10(1), p. 512. doi:
419 10.1038/s41467-019-08377-w.
- 420 Hamady, M., Lozupone, C. and Knight, R. (2010) 'Fast UniFrac: facilitating high-throughput
421 phylogenetic analyses of microbial communities including analysis of pyrosequencing and
422 PhyloChip data', *The ISME journal*, 4(1), pp. 17–27.
- 423 Hillmann, B. *et al.* (2018) 'Evaluating the Information Content of Shallow Shotgun
424 Metagenomics', *mSystems*, 3(6). doi: 10.1128/mSystems.00069-18.
- 425 Hugerth, L. W. and Andersson, A. F. (2017) 'Analysing Microbial Community Composition
426 through Amplicon Sequencing: From Sampling to Hypothesis Testing', *Frontiers in microbiology*,
427 8, p. 1561. doi: 10.3389/fmicb.2017.01561.
- 428 Jiang, H. *et al.* (2014) 'Skewer: a fast and accurate adapter trimmer for next-generation
429 sequencing paired-end reads', *BMC Bioinformatics*. doi: 10.1186/1471-2105-15-182.
- 430 Kembel, S. W. *et al.* (2011) 'The phylogenetic diversity of metagenomes', *PloS one*, 6(8), p.
431 e23214. doi: 10.1371/journal.pone.0023214.
- 432 Li, J. *et al.* (2017) 'Gut microbiota dysbiosis contributes to the development of hypertension',

- 433 *Microbiome*, 5(1), p. 14. doi: 10.1186/s40168-016-0222-x.
- 434 Lloyd-Price, J. *et al.* (2017) 'Strains, functions and dynamics in the expanded Human
435 Microbiome Project', *Nature*, 550(7674), pp. 61–66. doi: 10.1038/nature23889.
- 436 Louca, S., Doebeli, M. and Parfrey, L. W. (2018) 'Correcting for 16S rRNA gene copy numbers
437 in microbiome surveys remains an unsolved problem', *Microbiome*, 6(1), p. 41. doi:
438 10.1186/s40168-018-0420-9.
- 439 Lozupone, C. A. and Knight, R. (2008) 'Species divergence and the measurement of microbial
440 diversity', *FEMS microbiology reviews*, 32(4), pp. 557–578.
- 441 Lu, J. *et al.* (2017) 'Bracken: estimating species abundance in metagenomics data', *PeerJ*
442 *Computer Science*, p. e104. doi: 10.7717/peerj-cs.104.
- 443 Maiden, M. C. J. *et al.* (1998) 'Multilocus sequence typing: A portable approach to the
444 identification of clones within populations of pathogenic microorganisms', *Proceedings of the*
445 *National Academy of Sciences*, 95(6), pp. 3140–3145. Available at:
446 <http://www.pnas.org/content/95/6/3140.abstract>.
- 447 Matsen, F. A., 4th (2015) 'Phylogenetics and the human microbiome', *Systematic biology*, 64(1),
448 pp. e26–41. doi: 10.1093/sysbio/syu053.
- 449 Miller, C. S. *et al.* (2011) 'EMIRGE: reconstruction of full-length ribosomal genes from microbial
450 community short read sequencing data', *Genome biology*, 12(5), p. R44. doi:
451 10.1186/gb-2011-12-5-r44.
- 452 Obregon-Tito, A. J. *et al.* (2015) 'Subsistence strategies in traditional societies distinguish gut
453 microbiomes', *Nature communications*, 6, p. 6505. doi: 10.1038/ncomms7505.
- 454 Oksanen, J. *et al.* (2012) *vegan: Community Ecology Package*. Available at:
455 <http://CRAN.R-project.org/package=vegan>.
- 456 Orsi, W. D. (2018) 'Ecology and evolution of seafloor and subseafloor microbial communities',
457 *Nature reviews. Microbiology*, 16(11), pp. 671–683. doi: 10.1038/s41579-018-0046-8.
- 458 Ortiz-Álvarez, R. *et al.* (2018) 'Consistent changes in the taxonomic structure and functional
459 attributes of bacterial communities during primary succession', *The ISME journal*, 12(7), pp.
460 1658–1667. doi: 10.1038/s41396-018-0076-2.
- 461 Parks, D. H. *et al.* (2017) 'Recovery of nearly 8,000 metagenome-assembled genomes
462 substantially expands the tree of life', *Nature microbiology*, 2(11), pp. 1533–1542. doi:
463 10.1038/s41564-017-0012-7.
- 464 Parks, D. H. *et al.* (2018) 'A standardized bacterial taxonomy based on genome phylogeny
465 substantially revises the tree of life', *Nature biotechnology*, 36(10), pp. 996–1004. doi:
466 10.1038/nbt.4229.
- 467 Pasolli, E. *et al.* (2017) 'Accessible, curated metagenomic data through ExperimentHub',
468 *bioRxiv*. Cold Spring Harbor Laboratory. doi: 10.1101/103085.

- 469 Pericard, P. *et al.* (2018) 'MATAM: reconstruction of phylogenetic marker genes from short
470 sequencing reads in metagenomes', *Bioinformatics*, 34(4), pp. 585–591. doi:
471 10.1093/bioinformatics/btx644.
- 472 Royalty, T. M. and Steen, A. D. (2019) 'Quantitatively Partitioning Microbial Genomic Traits
473 among Taxonomic Ranks across the Microbial Tree of Life', *mSphere*, 4(4). doi:
474 10.1128/mSphere.00446-19.
- 475 Segata, N. *et al.* (2012) 'Metagenomic microbial community profiling using unique clade-specific
476 marker genes', *Nature methods*, 9(8), pp. 811–814. doi: 10.1038/nmeth.2066.
- 477 Sommer, F. and Bäckhed, F. (2013) 'The gut microbiota--masters of host development and
478 physiology', *Nature reviews. Microbiology*, 11(4), pp. 227–238. doi: 10.1038/nrmicro2974.
- 479 Torres, P. J. *et al.* (2018) 'Gut Microbial Diversity in Women With Polycystic Ovary Syndrome
480 Correlates With Hyperandrogenism', *The Journal of clinical endocrinology and metabolism*,
481 103(4), pp. 1502–1511. doi: 10.1210/jc.2017-02153.
- 482 Valles-Colomer, M. *et al.* (2019) 'The neuroactive potential of the human gut microbiota in
483 quality of life and depression', *Nature microbiology*. doi: 10.1038/s41564-018-0337-x.
- 484 Vogt, N. M. *et al.* (2017) 'Gut microbiome alterations in Alzheimer's disease', *Scientific reports*,
485 7(1), p. 13537. doi: 10.1038/s41598-017-13601-y.
- 486 Weimann, A. *et al.* (2016) 'From Genomes to Phenotypes: Traitair, the Microbial Trait Analyzer',
487 *mSystems*, 1(6). doi: 10.1128/mSystems.00101-16.
- 488 Wood, D. E., Lu, J. and Langmead, B. (2019) 'Improved metagenomic analysis with Kraken 2',
489 *Genome biology*, 20(1), p. 257. doi: 10.1186/s13059-019-1891-0.
- 490 Wu, M. and Scott, A. J. (2012) 'Phylogenomic analysis of bacterial and archaeal sequences with
491 AMPHORA2', *Bioinformatics*, 28(7), pp. 1033–1034. doi: 10.1093/bioinformatics/bts079.

492 Figure legends

493 **Figure 1.** *Similarity between phylogenetic and trait-based relatedness differs substantially*
494 *among phyla.* A) Traits inferred from each genome representative of each species, shown as
495 the percent of all genomes in the phylum (left) or the total for all phyla (right). The numbers next
496 to each column in the right plot denote the x-axis values. B) The boxplots show Procrustes
497 residuals for each genome, grouped by phylum. Higher Procrustes residuals indicate more
498 incongruence between phylogenetic and trait-based relatedness. For clarity, only phyla with ≥10
499 genomes are shown.

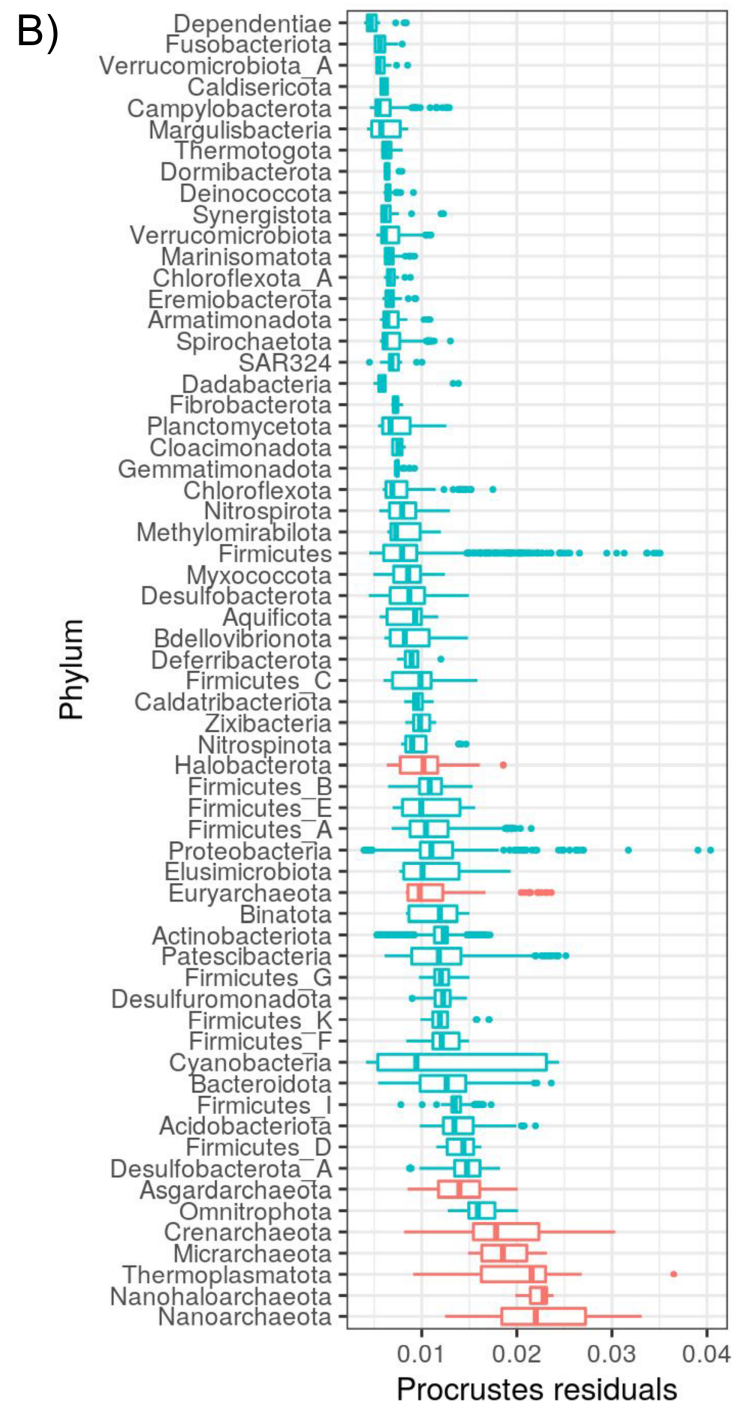
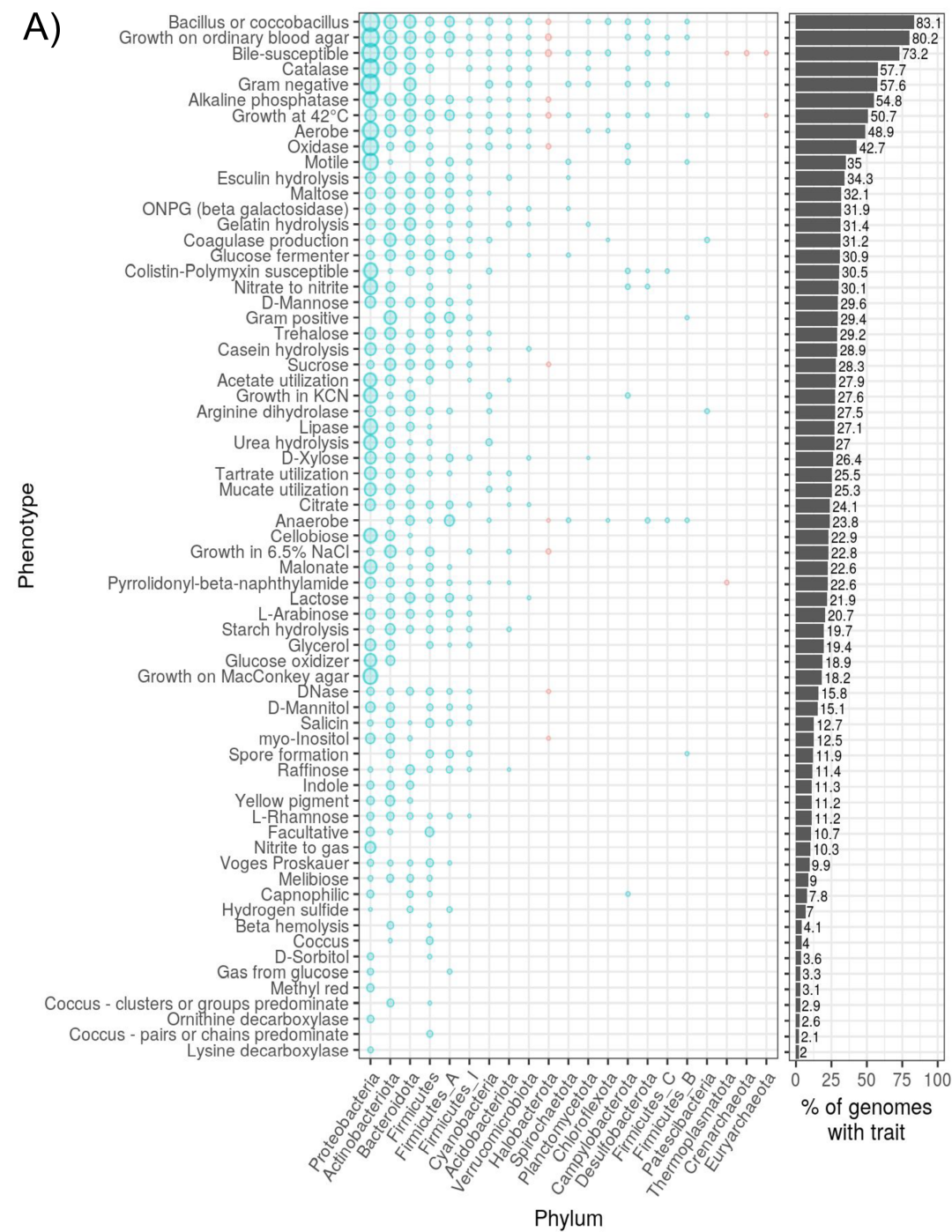
500 **Figure 2.** *Phylogeny- and trait-based alpha diversity better differentiate samples across key*
501 *factors.* A) Boxplots of alpha diversity metrics calculated for all samples ($n = 3348$) in all
502 datasets ($n = 33$), grouped by westernization status. "(phy)" denotes that the genome phylogeny
503 was used to calculate Faith's PD, while "(trt)" means that a dendrogram of trait similarity was

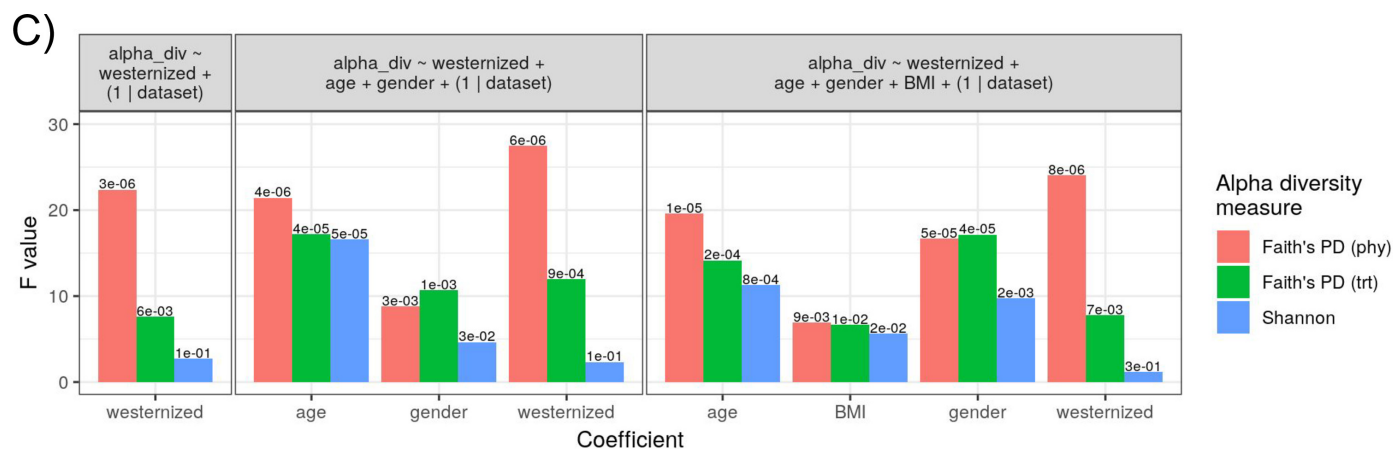
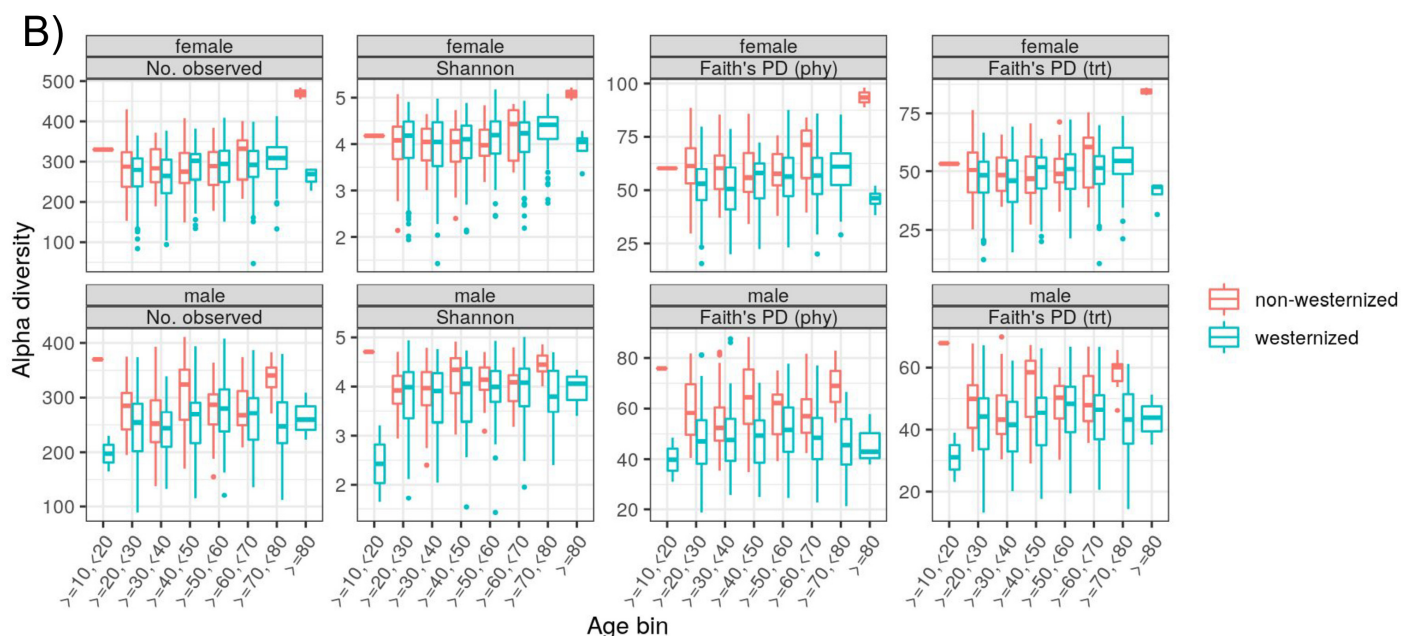
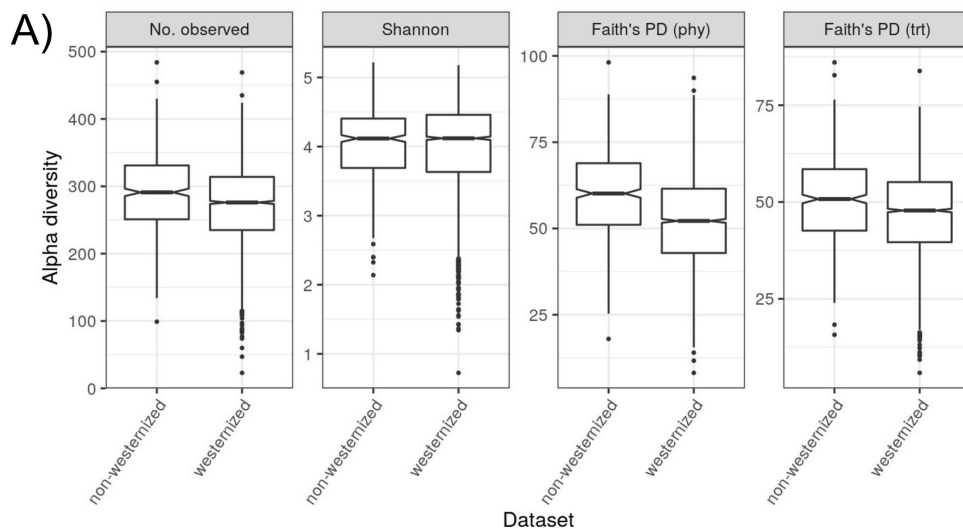
504 used for the calculation. B) Boxplots of alpha diversity metrics calculated for all samples in
505 which gender and age metadata were available ($n = 1843$) in all datasets ($n = 17$), grouped by
506 westernization of individuals. C) Linear mixed effects model results for assessing the
507 association between alpha diversity and population characteristics while accounting for
508 inter-dataset batch effects. The labels above each bar denote P -values. Age was
509 log2-transformed, and BMI Box-Cox transformed. The left facet is on all samples ($n = 3348$) in
510 all datasets ($n = 33$). The middle facet is filtered to samples that have data on gender and age
511 (number of samples = 1843; number of studies = 17). The right facet is filtered to samples that
512 have data on gender, age, and BMI (number of samples = 918; number of studies = 11).

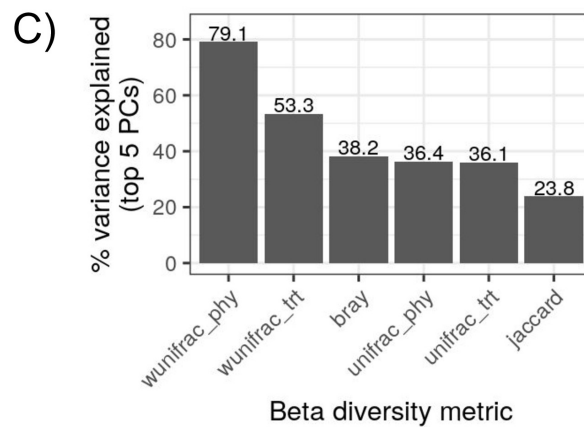
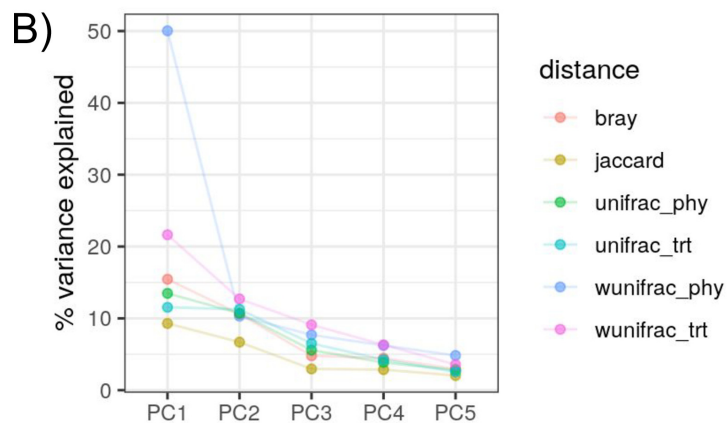
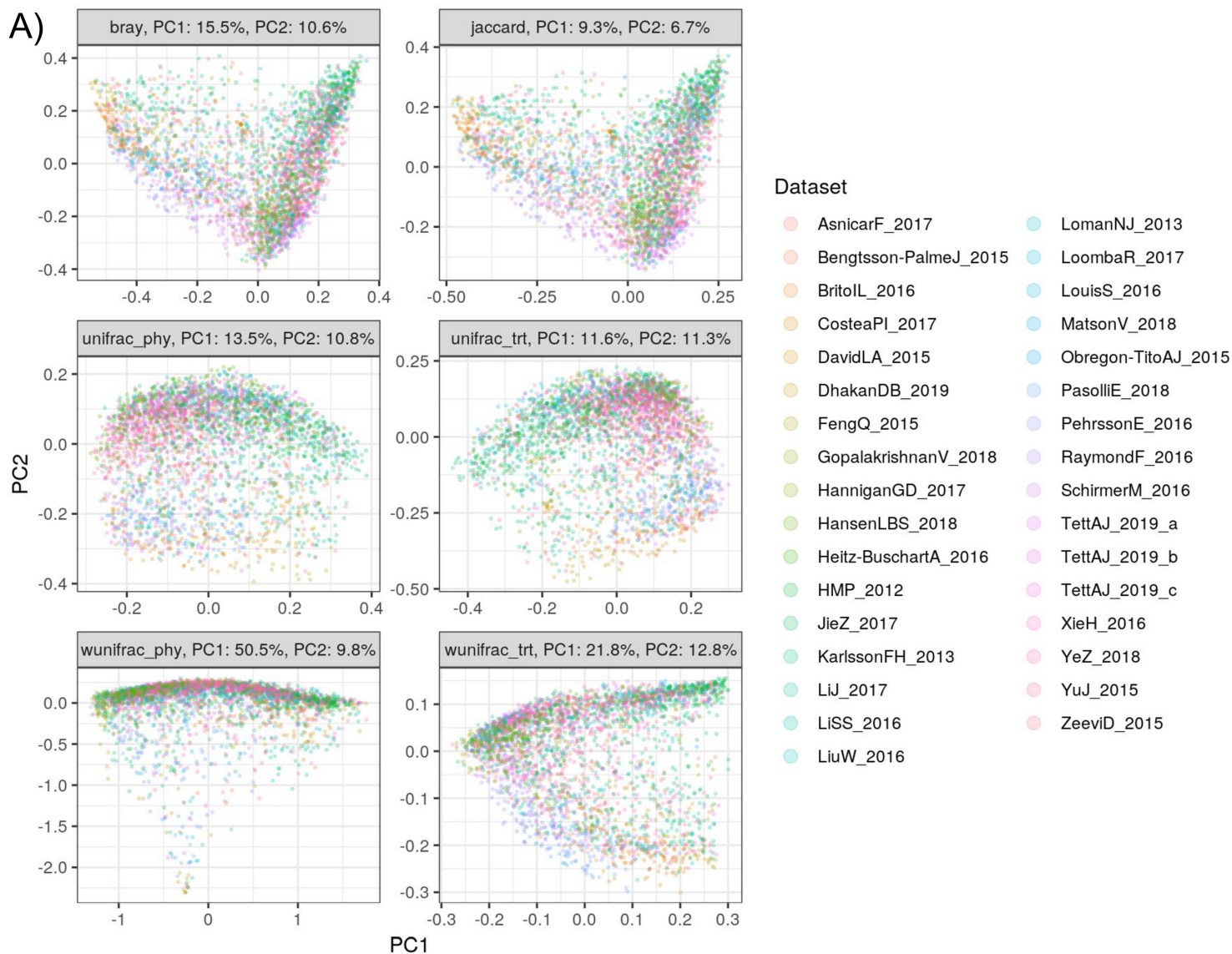
513 **Figure 3.** *More variance explained when incorporating taxon abundance along with*
514 *phylogenetic- or trait-based relatedness.* Principal coordinate analysis (PCoA) ordinations for all
515 samples across all datasets ($n = 3348$), colored by dataset and faceted by the beta-diversity
516 metric used (“bray” = Bray-Curtis; “jaccard” = Jaccard; “unifrac_phy” = unweighted UniFrac
517 utilizing the genome phylogeny; “unifrac_trt” = unweighted UniFrac utilizing a dendrogram
518 depicting trait-similarity; “wunifrac_phy” = “unifrac_phy”, but using weighted UniFrac;
519 “wunifrac_trt” = “unifrac_trt”, but using weighted UniFrac). The percentages in each facet label
520 are the percent variance explained for the first two PCs. B) The percent variance explained by
521 the top five PCs for each ordination shown in A). C) The summed percent variance explained by
522 the top five PCs for each ordination shown in A), with values above each bar denoting the y-axis
523 value.

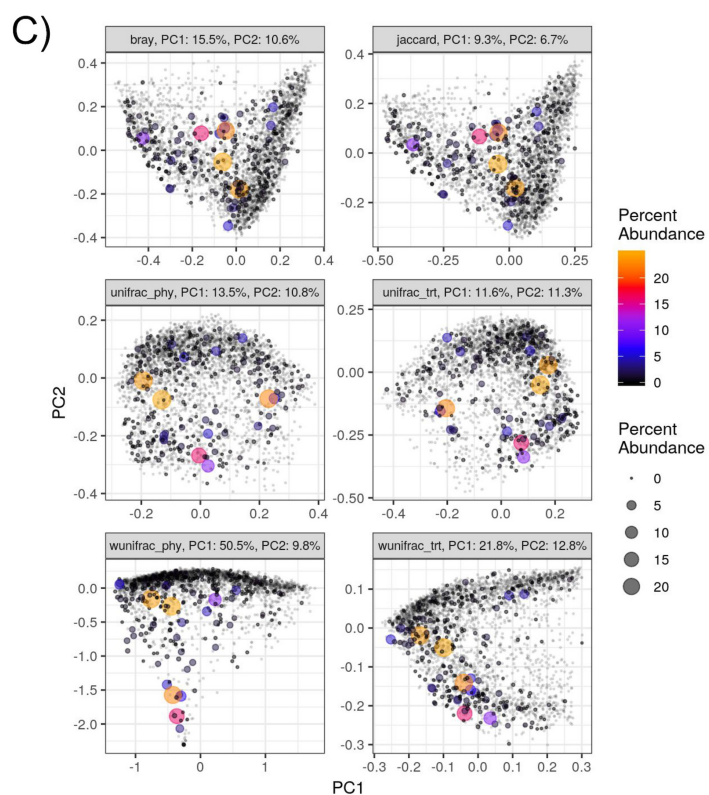
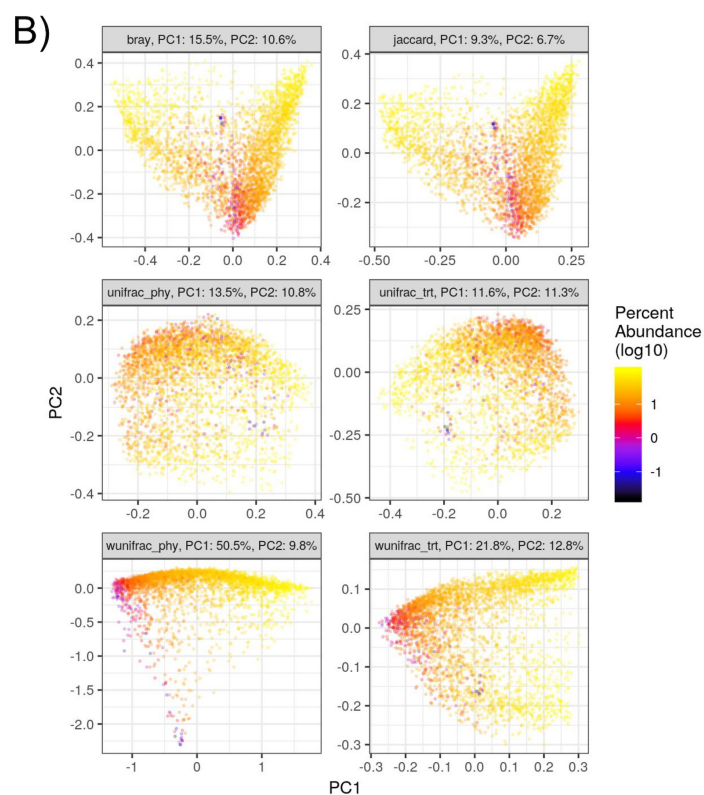
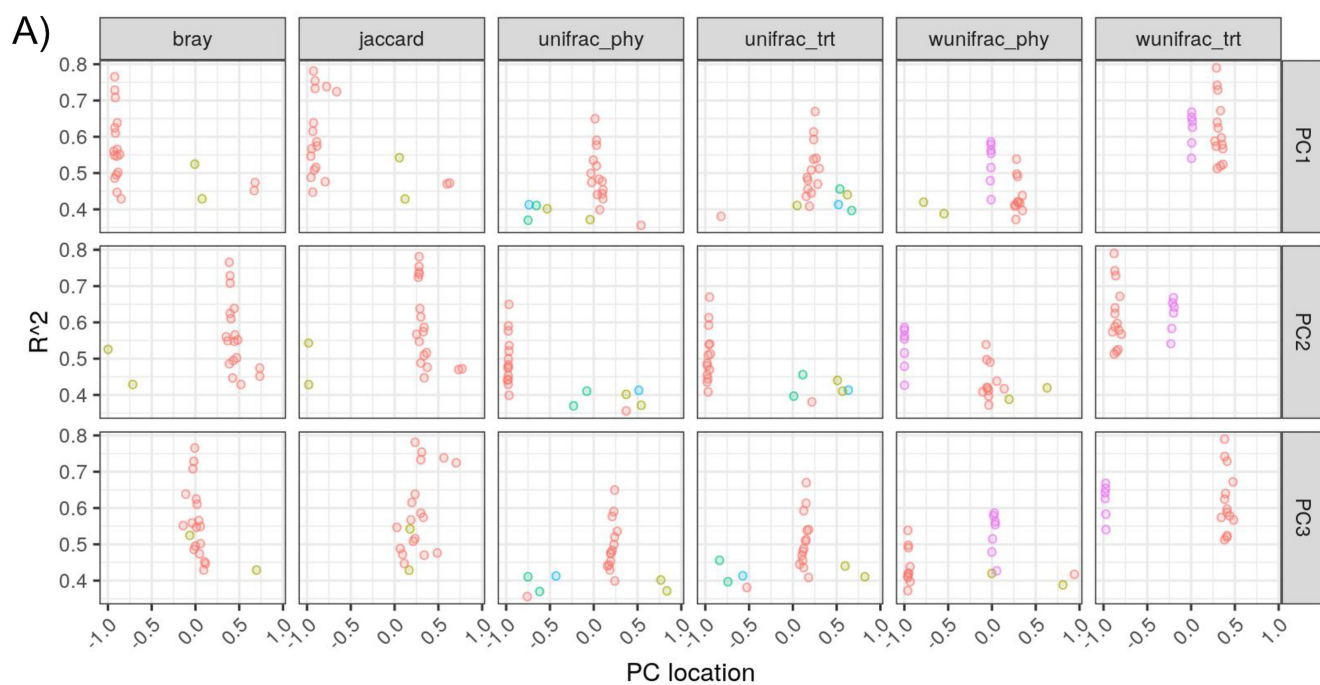
524 **Figure 4.** *Phylogeny- and trait-based beta-diversity metrics emphasize inter-sample differences*
525 *in certain taxa that are not emphasized by star-phylogeny measures.* A) Correlations between
526 individual species (points) and the top 3 PCs in the PCoA ordinations shown in Figure 3. The
527 x-axis denotes the direction of the correlation along the PC (*i.e.*, where the taxon abundance is
528 highest), and the y-axis denotes the effect size. For clarity, only species with the top 20 highest
529 effect sizes across all beta diversity metrics are shown. The PCoA ordinations shown in B) and
530 C) are the same as in Figure 3, but samples are colored by the abundance of the
531 *Bacteroidaceae* family (*Bacteroidota* phylum) and *Enterobacteriaceae* (*Proteobacteria* phylum),
532 respectively. Note that abundance is not log10-transformed in C), and point size also represents
533 abundance in order to emphasize the few samples with relatively high *Enterobacteriaceae*
534 abundances, and all grey points indicate samples completely lacking *Enterobacteriaceae*.

535 **Figure 5.** *UniFrac-based beta diversity better explains disease status across the metagenome*
536 *dataset.* A) Variance explained for each covariate in PERMANOVA models ($n = 1413$) applied to
537 each distance matrix as shown in PCoA plots in Figure 3. B) The position of each sample
538 (grouped by disease state) on PC1 for each PCoA of each beta diversity measure as shown in
539 Figure 3. Note that for the tree-agnostic approaches, most disease states fall into the same,
540 constrained range; however, the UniFrac-based approaches (especially weighted UniFrac)
541 generate more separation among disease groups (“STEC” = Shiga toxin-producing *E. coli*;
542 “T2D” = Type 2 diabetes; “ACVD” = atherosclerotic cardiovascular diseases; “CMV” =
543 Cytomegalovirus disease, “IGT” = impaired glucose tolerance). All terms in each PERMANOVA
544 model were significant (number of permutations = 9999; $P < 0.001$).

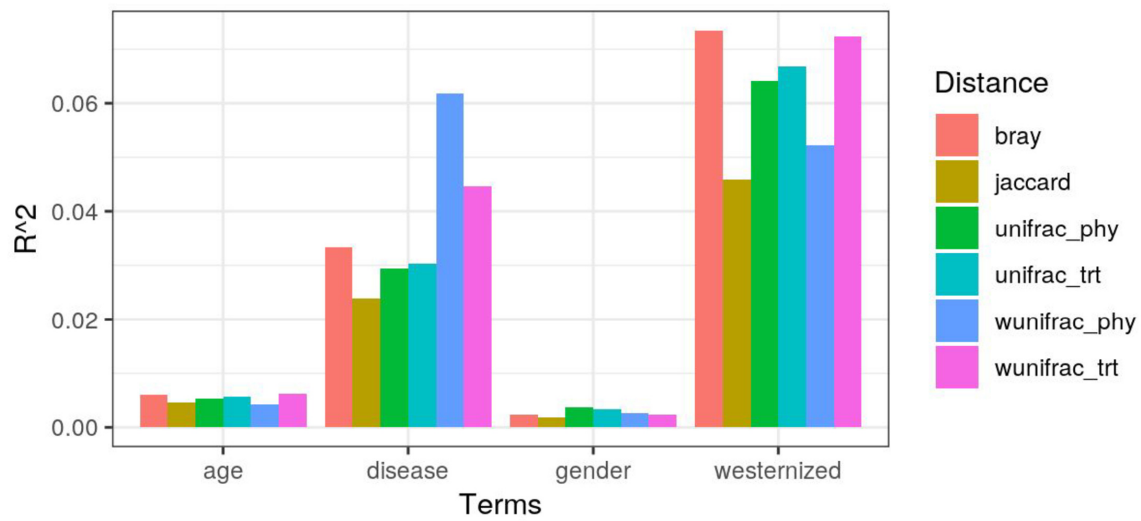








A)



B)

